A new ZVT power factor corrected three-phase AC-AC converter with single-phase HF link

Ahmad J. Sabzali and Tamer H. Abdelhamid
College of Technological Studies, Kuwait

This paper presents a new Zero-Voltage Transition (ZVT), power factor corrected three-phase ac-ac converter with single-phase High Frequency (HF) link. It is a two-stage converter; the first stage is a boost-integrated bridge converter (combination between 3-ph boost converter and a bridge converter) operated at fixed frequency and operates in two modes at ZVT for all switches and establishes a 1-ph square wave HF link. The second stage is a bi-directional Pulse-Width Modulation (PWM) 3-ph bridge that converts the 1-ph HF link to a 3-ph voltage using a novel switching strategy. The converter modes of operation and key equations are outlined. Simulation of the overall system is carried out using Simulink. The switching strategy and its corresponding control circuit are clearly described. Experimental verification of the simulation is carried out for a prototype of 100V, 500W at 10kHz link frequency.

يقدم هذا البحث دائرة جديدة لمحول تيار متردد– تيار متردد ثلاثي الأوجه بانتقال صفري للجهد ومعامل قدرة محسن ووصلة عالية التردد أحادية الوجه. يتكون المحول من مرحلتين – المرحلة الأولى عبارة عن قنطرة مدمجة بمثبت جهد تعمل على تردد ثابت بنمطين تشغيل عند انتقال صفري للجهد لجميع مفاتيح أشباه الموصلات و تنشئ موجة مربعة أحادية الوجه عالية التردد. المرحلة الثانية عبارة عن قنطرة ثلاثية الأوجه مكونة من مفاتيح أشباه مواصلات ثنائية الاتجاه و تعمل باستراتيجية مبتكرة – يعرض البحث أنماط التشغيل والمعادلات الأساسية للدائرة، كما يقدم البحث دائرة التحكم المستخدمة و تمثيل النظام الكلي على الحاسب الآلي باستخدام حزمة برامج simulink وكذلك عرض للنتائج المعملية التي تم الحصول عليها من نموذج معملي للدائرة بقدرة ٥٠٠ وات و وصلة عالية التردد ١٠ كيلوهرتز.

Keywords: Zero-Voltage Transition (ZVT), Power Factor Correction (PFC), AC-AC converter

1. Introduction

Power Factor Correction (PFC) circuits have become standard input stages for almost every medium and high power switching power supply operating at the mains voltage. Today's most often used configuration includes a boost converter as an input stage, stabilizing the input to the second stage, which is usually a half- or full-bridge converter which provides all necessary output voltages [1]. Efficiency of the boost PFC is high (90-95%), but the second stage converter has a maximum efficiency of about 85% (which is significantly reduced if high output currents are produced). Overall maximum efficiency is, therefore, about 76%-80% [2].

Recently, soft-switching techniques are used to eliminate variable frequency operation, reduce component stress and improve the system efficiency. Zero-Voltage Transition and Zero-Current Transition (ZVT and ZCT) modifications of almost every basic converter topology have been widely accepted, and the semiconductor industry has followed that trend by developing several fully integrated controllers. The full-bridge, phase-shift, ZVS topology is the most frequently used [3].

A non-sinusoidal voltage clamper circuit has been used to achieve soft switching with an inductive or current source load. However, excessive voltage stress due to the leakage inductance (typically about 4 times the input line voltage) has been reported [4].

Numerous ZVT converter topologies have been previously proposed [5, 6], however these drawbacks have been reported:

1. The auxiliary circuit consists of several components, and the auxiliary switch requires a floating gate drive.
2. The auxiliary circuit components have high voltage and current stresses and therefore, increased conduction losses.
3. Reduced overall efficiency due to the hard turn-off of the auxiliary switch.

To overcome these drawbacks, several kinds of soft switching PWM converters have been presented in the literature [7, 8]. They achieve high efficiency, minimum switching stresses, switching losses, and facilitate PWM control with constant frequency operation. All soft switching PWM methods utilize resonant techniques to soften the switching transition with Zero-Voltage Switching (ZVS and/or (Zero-Current Switching) ZCS, and they can be generally classified into either passive or active ones. Passive methods use only resonant inductors, capacitors, and diodes to achieve soft switching turn-on and/or turn-off of the switches [9]. Active methods, as in [4], use resonant inductors, capacitors, diodes, and auxiliary active switches to reduce switching loss due to main power switches. The concepts of fundamental soft switching cells were employed to generate many families of soft switching PWM converters [7-11].

The ZVT-PWM soft-switching converters [10, 11] solve the existing problems of high switching losses of conventional PWM converters and high voltage and current stresses of resonant converters. These kinds of converters are especially useful in the application of high efficiency power converter systems.

This paper presents a new ZVT, power factor corrected three-phase ac-ac converter with single-phase HF link. The proposed system configuration enjoys the following advantages: switching at ZVT, input PFC, constant frequency operation, and single-phase HF link that makes it possible to use a single-phase isolation transformer if isolation is needed for the system. The different modes of operation, switching strategy, and control circuit are presented. Results obtained from Simulink simulation of a 500W, 100V laboratory prototype switching at 10kHz, verify the performance of the proposed configuration, highlight its advantages, and mention its drawbacks.

2. Circuit description and operation

The detailed circuit diagram of the proposed 3-ph ac-ac converter employing input PFC and ZVT is shown in fig. 1. The proposed system consists mainly of two converters; the first converter is a combination of a 3-ph boost converter and a bridge converter, its function is to establish the constant amplitude-constant frequency 1-ph HF link voltage at ZVT for the bridge converter switches, and incorporates the input PFC of the 3-ph supply currents. The second converter is a 3-ph PWM bi-directional bridge, its function is to reconstruct a balanced 3-ph low frequency output voltage from the constant amplitude-constant frequency 1-ph HF link voltage. A 3-ph filter is located at the 3-ph bridge's terminals in order to suppress the associated switching harmonics. A HF isolation transformer is included in the circuit for galvanic isolation of the dc side from the load circuit.

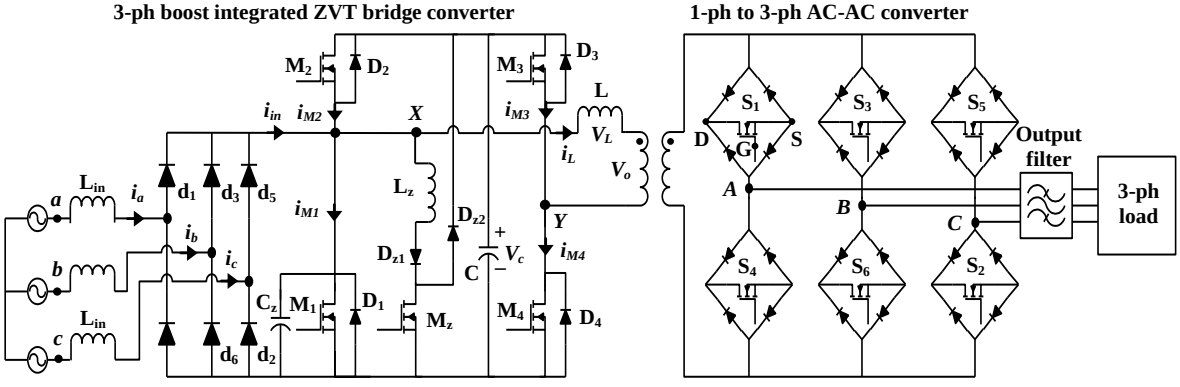

Fig. 1. The proposed ZVT power factor corrected 3-ph AC-AC converter with 1- 1-ph HF link.

2.1. The boost integrated ZVT converter

This converter can be operated in Continuous Current Mode (CCM) or in Discontinuous Current Mode (DCM) depending on the loading conditions. In CCM, the gating signals of switches $M_1 \rightarrow M_4$ have a 50% complementary duty cycle, and a square wave HF link is established. At light loads, the converter operates in DCM where pulse width is decreased with a dead gap and the HF link voltage is symmetrically cut by an angle α from both ends. The current waveform in the tank inductor is divided into several intervals for each mode of operation. These intervals depend on the polarity of voltage and direction of current in the tank circuit.

The equivalent circuits during different time intervals are shown in fig. 2. Note that the HF cycle is completed during the interval when d_1, d_2 and d_6 are conducting. In CCM, the modes of operation can be summarized as follows: the cycle starts when diodes D_1 and D_3 are conducting, fig. 2-a, inductor current decreases from its initial value and before the end of this interval switch M_1 is turned-on at ZVT, then current in diode D_1 transfers to switch M_1, fig. 2-b. The input inductors, L_{in}, prevent the momentary short-circuit which occurs across the supply, as in conventional 3-ph boost converter. When switch M_3 conducts at ZVT, the current in diode D_3 transfers to the switch M_3, fig. 2-c.

$$i_L(t) = i_L(t_o) - \frac{(V_c - V_o)}{L}(t - t_o). \quad (1)$$

$$V_{XY} = V_L - V_o, \quad (2)$$

$$i_{M1}(t) = i_{in}(t) - i_L(t), \quad (3)$$

$$i_{M3}(t) = -i_L(t). \quad (4)$$

Switches M_1 and M_3 are turned-off when diodes D_2 and D_4 become forward biased, fig. 2-d. When the current in diode D_4 transfers to M_4 at ZVT, fig.2-e, inductor current becomes negative and increases linearly; when switch M_2 turns-on ZVT, diodes D_2 and D_4 become reverse biased, and the link voltage equals the capacitor voltage, fig. 2-f.

$$i_L(t) = \frac{(V_c - V_o)}{L}(t - t_2) + i_L(t_2). \quad (5)$$

$$V_{XY} = V_c, \quad (6)$$

$$i_{M2}(t) = i_L(t) - i_{in}(t), \quad (7)$$

$$i_{M4}(t) = i_L(t). \quad (8)$$

If overlap of triggering signals exists, the following interval will be added to the previous intervals. This interval happens when diode D_3 becomes forward biased, and switch M_4 turns-off, fig. 2-g, inductor current decreases linearly from its initial condition; the inductor current keeps decreasing as long as both switch M_2 and diode D_3 are conducting, and the link voltage becomes zero, fig. 2-h.

$$i_L(t) = i_L(t_4) - (V_o / L)(t - t_4). \quad (9)$$

$$V_{XY} = 0, \quad (10)$$

$$i_{M2}(t) = i_L(t) - i_{in}(t), \quad (11)$$

$$i_{M3}(t) = -i_L(t). \quad (12)$$

In DCM, the modes of operation can be summarized as follows: the cycle starts when diode D_1 is conducting, the current in D_1 is a resonating sinusoid with a maximum value of $V_c / \sqrt{L_z / C_z}$, that provides the ZVT for switch M_1, in addition to D_3, switch M_3 and the auxiliary switch M_z are conducting, and the HF link voltage equals to the negative of the capacitor voltage, fig. 2-i. When switch M_1 turns-on at ZVT, the current in M_1 increases until the end of this interval while the inductor current decreases linearly, where the HF link voltage still equals the negative of the capacitor voltage,

$$i_L(t) = -\frac{(V_c - V_o)}{L}(t - t_1), \quad (13)$$

$$V_{XY} = -V_c. \quad (14)$$

$$i_{M1}(t) = i_{in} - i_L(t), \quad (15)$$

$$i_{M3}(t) = -i_L(t). \quad (16)$$

The following three intervals are the same as those of CCM except that at the end of the last interval, currents in M_2, D_3, and inductor

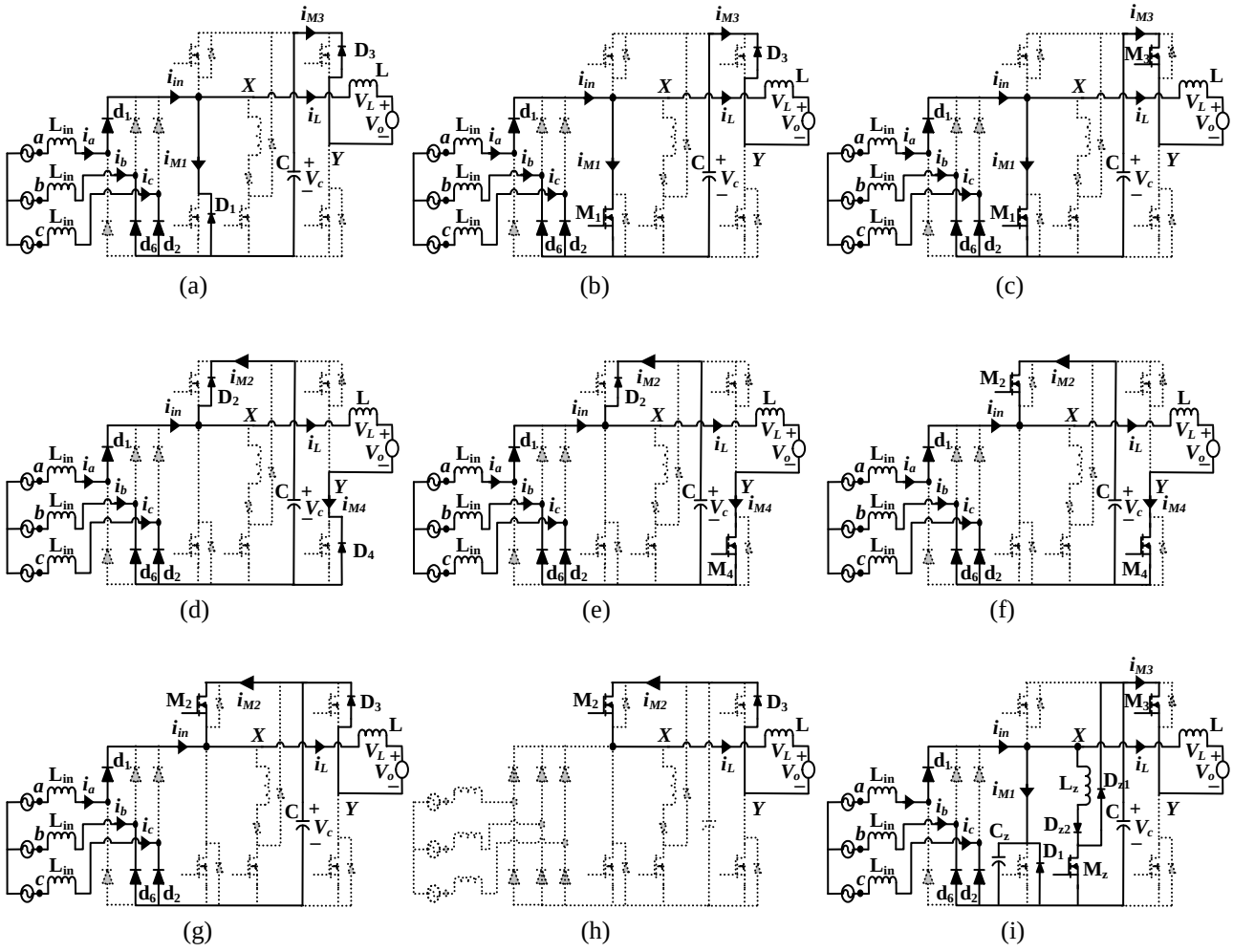

Fig. 2. Equivalent circuits for the different time intervals of the 3-ph boost-integrated ZVT bridge converter.

are all equal to zero, and the HF link voltage becomes zero due to the overlap between triggering signals of M_2 and M_3.

2.2. The1-Ph to 3-Ph AC-AC converter

Since the output of the bridge converter is of a constant amplitude, the modulation process should be incorporated in the output stage. Therefore, the output ac-ac converter should be controlled by a certain PWM technique in order to achieve the modulation process of the overall system.

The complete switching strategy of the 1-ph to 3-ph ac-ac converter is illustrated in fig. 3. The PWM control strategy is carried out by switching signal generation circuit where a carrier triangular waveform having a frequency much greater than that of the output voltage is compared with 3-ph reference sine-wave signals synchronized with the mains supply. The ratio of the frequencies of the triangle wave and the reference sine waves is defined as the frequency modulation ratio M_f. This ratio is typically in order of 200-400 for HF link applications. However, this ratio is taken as 9 in fig. 3 in order to provide clear illustrating waveforms. The ratio of the amplitude of the sine and carrier waveforms is known as the amplitude modulation index, M_a, as it provides the modulation process of the amplitude of the output voltage. For linear modulation region, this value is restricted from 0 to 1 and it is

taken as 0.8 in fig. 3. The control strategy of the 1-ph to 3-ph ac-ac converter can be summarized as follows: a signal is taken from one of the phase voltages of the mains supply, where the other two signals of the following two phases are obtained via two cascaded phase shifting circuits such that control signals F_1, F_2, and F_3 are obtained. The outputs of the three comparators are denoted F_a, F_b, and F_c respectively. These signals are used to derive the 3-ph line voltages signals through subtracting circuits such that F_{ab}, F_{bc}, and F_{ca} are obtained. F_d is the derivative of the carrier waveform. The switching patterns of the 1-ph to 3-ph ac-ac converter $G_1 \rightarrow G_6$ are synthesized as follows: The individual pulses of the F_{ab} are alternately carried by switch pairs S_1, S_6 and S_3, S_4, while the pulses of F_{bc} are alternately carried by S_5, S_6 and S_3, S_2, and the pulses of F_{ca} are alternately carried by S_5, S_4 and S_2, S_1. The pulses carried by switch pairs S_1, S_6 and S_3, S_4 for F_{ab} can be obtained by multiplying F_{ab} by F_d, such that the switching signal G_{ab} is obtained. Another two signals G_{bc}, and G_{ca} are also obtained by multiplying F_{bc}, and F_{ca} by the F_d. This step identifies the switching pulses of each pair of switches S_1 and S_6 (G_{16}: the positive pulses of G_{ab}), and the switching pulses of the pair of switches S_3 and S_4 (G_{34}: the negative pulses of G_{ab}). This step is repeated for the F_{bc} and F_{ca} such that another four sets of gating signals are obtained, namely G_{12}, G_{32}, G_{56}, and G_{54}. The total switching pattern of each switch is the aggregate of the pulses carried out by the switch to supply different line voltage. This can be obtained by *ORing* the switching patterns accomplished by the same switch for different line voltages (for example; $G_1=G_{16}$ *OR* G_{12}). The final switching patterns of the 1-ph to 3-ph ac-ac converter $G_1 \rightarrow G_6$ shows that they possess a half-wave symmetry where the switches in the same arm don't conduct at the same time to avoid short-circuiting the transformer terminals. This switching strategy can be applied for any value of M_f (odd or even) and also, not necessarily to be a multiple of three as required by conventional switching strategies.

The control circuit used to verify this switching strategy is shown in fig. 4. It consists of 3 comparators to obtain F_a, F_b, and F_c; 3 subtracting circuits to get the 3 line voltages signals F_{ab}, F_{bc}, and F_{ca}; 3 multipliers to get the 3 functions G_{ab}, G_{bc}, and G_{ca}; 3 negative clippers to get G_{16}, G_{32}, and G_{54}; and 3 inverting amplifiers followed by 3 negative clippers to get G_{34}, G_{56}, and G_{12}. Then 6 OR gates to obtain

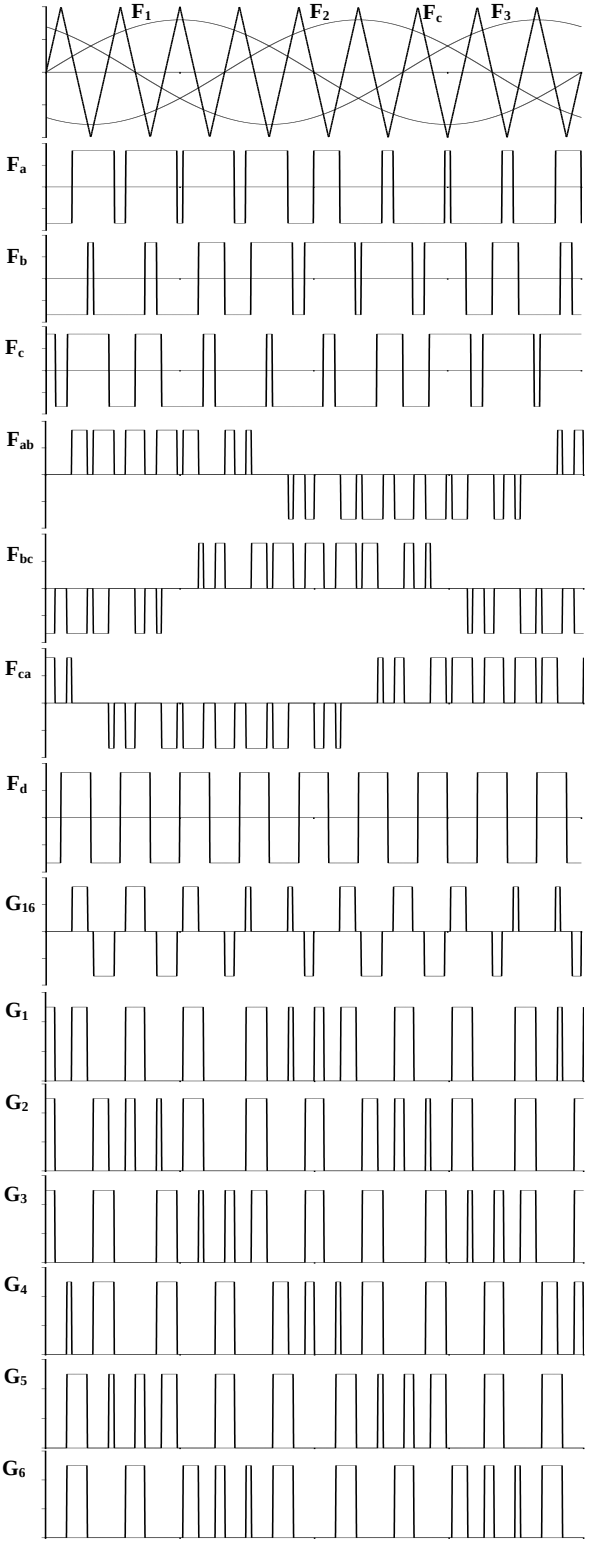

Fig. 3. Switching strategy of the 1-ph to 3-ph ac-ac converter.

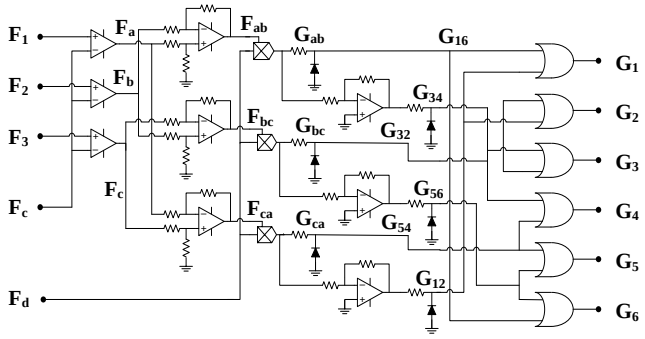

Fig. 4. Control circuit of the PWM 1-ph to 3-ph AC-AC converter.

3. Simulink simulation

In order to verify the validity of the proposed system, the overall system is simulated using Simulink. A design example at 10kHz switching frequency is chosen in order to save the disc space and shorten the computation time. The Simulink connection diagram is shown in appendix A. The selection of the values of circuit elements is based on solving the steady-state relations of the described modes of operation at full-load. The full load rating of the design example is chosen at 500W, and 100V HF link.

Typical simulation waveforms at full-load for 50% duty cycle and CCM are shown in fig. 5. The waveforms are presented in the following order: the switching patterns of switches $M_1 \rightarrow M_4$; HF link voltage, inductor current; and current in M_3 and M_4. The negative parts of switch current are carried by its corresponding anti-parallel diode. Another set of simulation waveforms at light load in DCM are shown in fig. 6 for 30% duty cycle, where an overlap between switching signals occurs, and a dead interval in the HF link voltage is observed. It can be shown that the ZVT is achieved during the entire range of load variation.

The un-rectified 3-ph output phase and line voltages are shown in figs. 7-a and 7-b respectively, where the validity of the switching strategy of the 1-ph to 3-ph ac-ac converter is verified. The 30° phase angle between each line voltage and its corresponding phase voltage can also be observed. An expanded waveform of V_A, V_B and V_{AB} is shown in fig. 7-c. The harmonic spectrum of the output phase and line voltages are shown in fig. 8, where the associated harmonics appear at the link frequency and its multiples. The 3-phase input voltages and currents are shown in fig. 9, where high quality input current waveforms are obtained with nearly unity power factor. This reflects the effectiveness of the PFC boost-integrated ZVT converter.

4. Experimental verification

In order to verify the feasibility of the proposed converter, a 500W, 100V prototype is designed and built for illustration purpose at 10kHz link frequency. The available MOSFET switches IRF840A (500V-8A) are used as the main controlled switches, and fast recovery diodes MUR860 (600V-8A) are used in the whole system. The circuit parameters details are: supply voltage: 100V, 50Hz, L_{in}=1mH, L_z=22μH, C_z=1μF, C=470μF, and L=47μH (including HF transformer leakage inductance), turns ratio of the HF transformer=1, and a variable resistive load is used to draw a load power up to 500W. The voltage and current of switches M_1 and M_2 at 50% duty cycle for CCM are shown in figs. 10 and 11 respectively. The traces of M_3 and M_4 are similar to those of M_1 and M_2 respectively. The voltage and current of switch M_z are shown in fig. 12. The corresponding inductor current I_L and the HF link voltage V_{XY} are shown in figs. 13 and 14 respectively. The voltage and current of switch M_1 in the DCM is shown in fig. 15. It can be seen that the boost-integrated ZVT converter operates with ZVS for all switches. The gating signals of switches $S_1 \rightarrow S_6$ are shown in figs. 16, and 17. The unfiltered 3-ph output voltages are shown in fig. 18, where the output

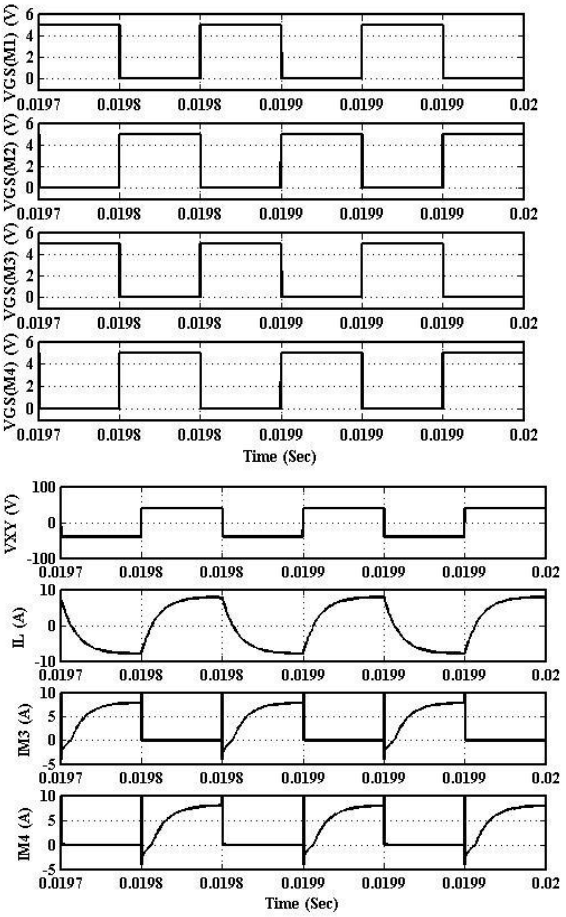

Fig. 5. Simulink simulation waveforms of the CCM of the boost-integrated ZVT converter.

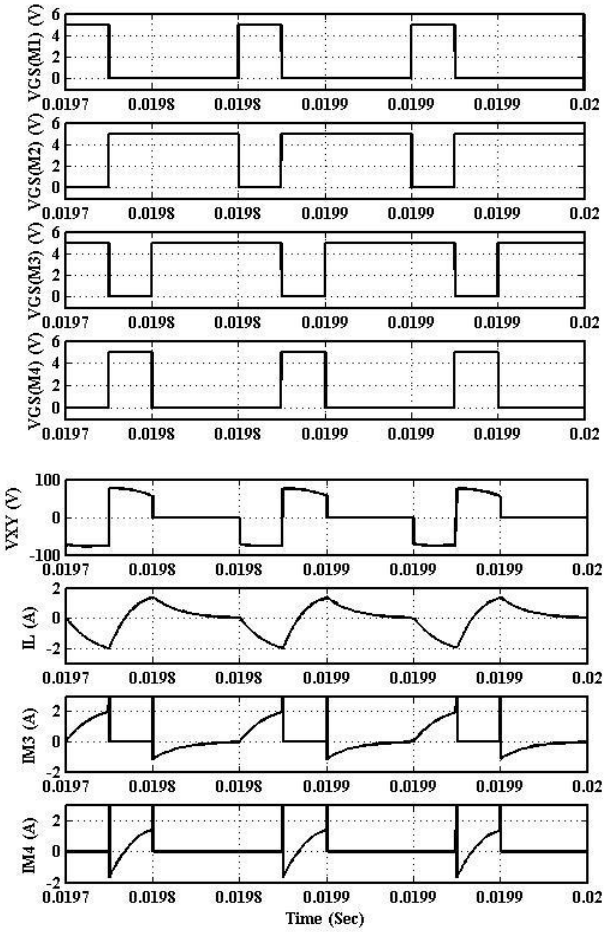

Fig. 6. Simulink simulation waveforms of the DCM of the boost-integrated ZVT converter.

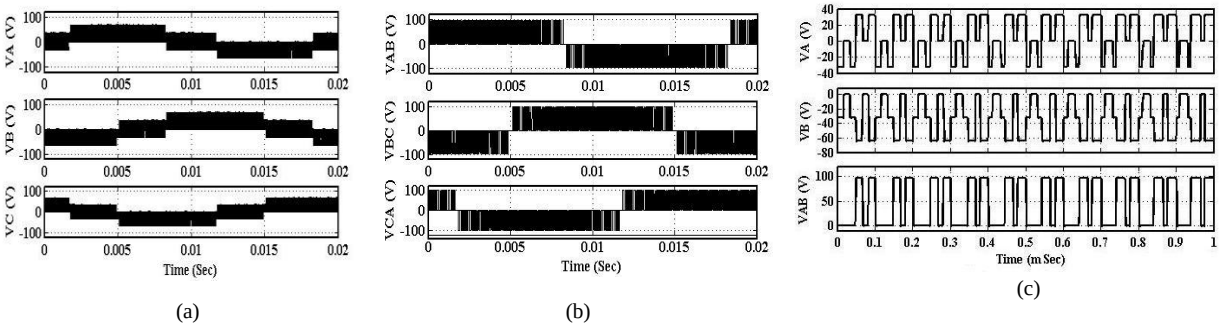

Fig. 7. The output waveforms of the 1-ph to 3-ph AC-AC converter a- phase voltages, b- line voltages, c- expanded waveform.

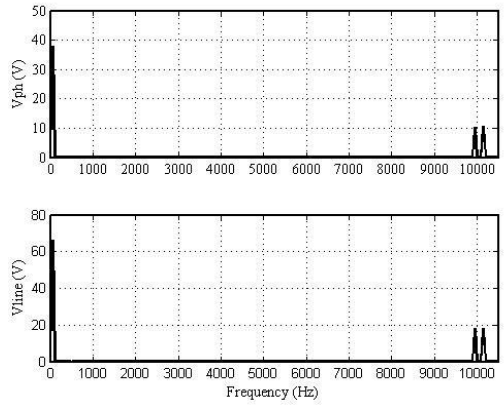

Fig. 8. Harmonic spectrum of output phase and line voltages.

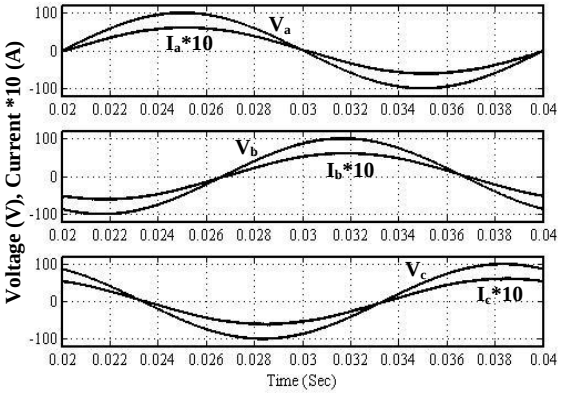

Fig. 9. The 3-phase supply input phase voltages and currents.

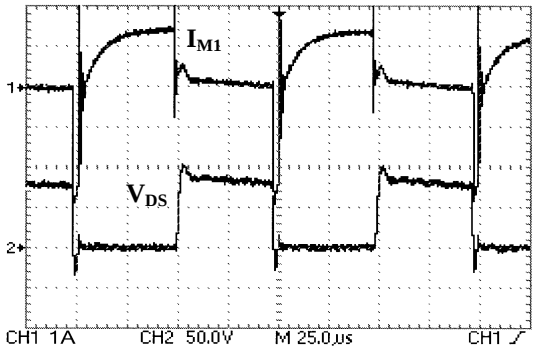

Fig. 10. Voltage and current of switches M_1 in CCM.

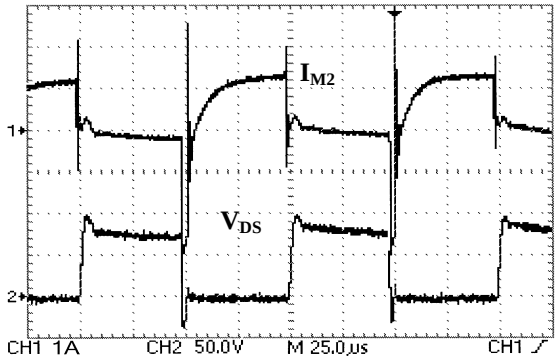

Fig. 11. Voltage and current of switches M_2 in CCM.

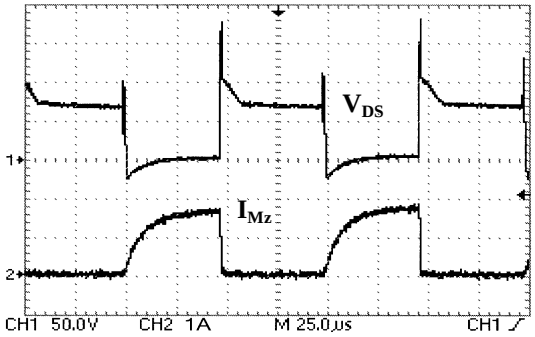

Fig. 12. Voltage and current of switches M_z in CCM.

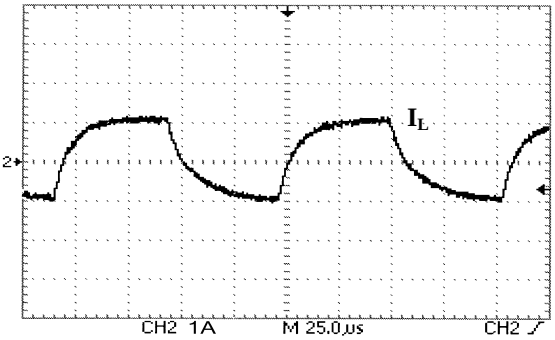

Fig. 13. The inductor current in CCM.

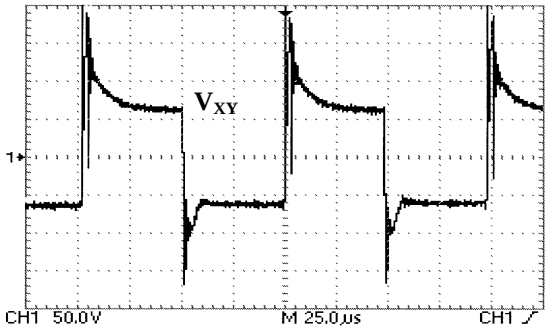

Fig. 14. The HF link voltage in CCM.

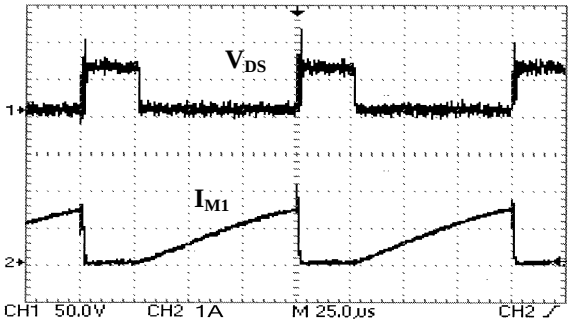

Fig. 15. Voltage and current of switch M_1 in DCM.

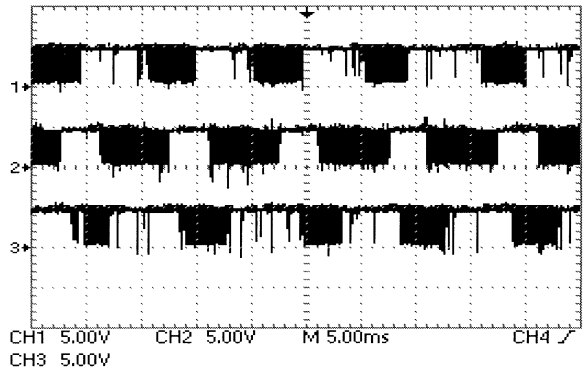

Fig. 16. The gating signals of switches S_1, S_2, and S_3.

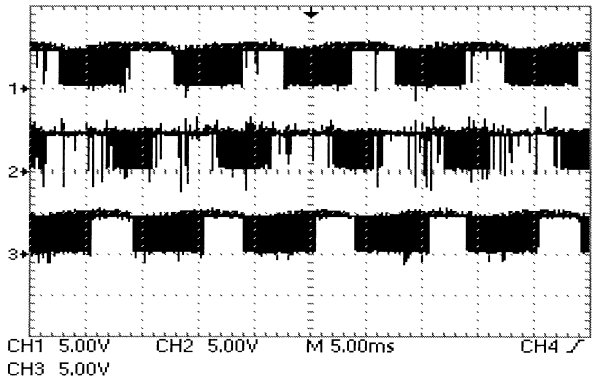

Fig. 17. The gating signals of switches S_4, S_5, and S_6.

voltages have a low-frequency profile modulated at the 10kHz link frequency. Its harmonic spectrum is shown in fig. 19, where it has its fundamental component at 50Hz and the first dominant harmonics appear at the link frequency, 10kHz, which can be easily filtered out using small size output filter. The supply input voltage and current of one of the input phases are shown in fig. 20, where the input current is sinusoidal and in-phase with the input voltage. It can be also seen that the experimental results are in close agreement with the presented simulation results. The measured power factor ranges around 0.98 during the entire range of load variation (0→500W). However, the overall system efficiency is about 88% due to the high on-resistance of the MOSFETs used, and the PWM nature of the 1-ph to 3-ph ac-ac converter.

5. Conclusions

A new configuration of 3-phase ac-ac converter has been proposed. The proposed system is based on a single-stage boost integrated ZVS converter, a 1-ph HF link, and a 1-ph to 3-ph ac-ac converter to reconstruct the low frequency output voltage. The overall system operates at a fixed frequency PWM control scheme, where synchronization between input and output voltages is taken into account through control circuit. Key equations, simulation and experimental results have been presented. ZVS is ensured for all switches of the input stage, for the two modes of operation during the entire range of load variation. The novel switching strategy of the 1-ph to 3-ph AC-AC converter is verified

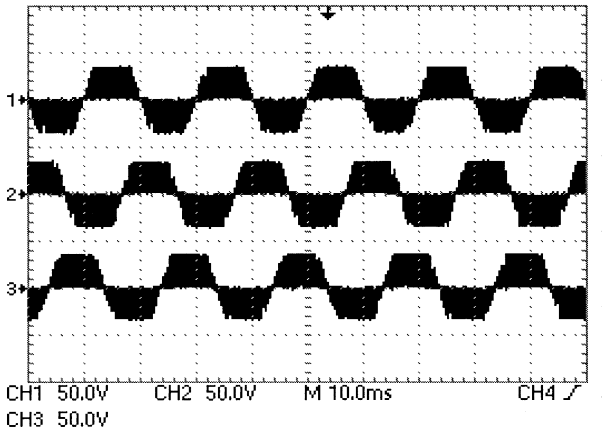

Fig. 18. The un-filtered 3-phase output voltages.

experimentally, where the output harmonics appear at the link frequency. However, the system has the disadvantage that the harmonic content of the HF link is quit high due to its square wave nature, this will affect the design of the HF transformer. This can be prevailed by making the HF link has a sinusoidal nature, which, in turn, will affect the ZVS converter configuration. Also, the PWM nature of the output ac-ac converter lowers the overall system efficiency. Applying soft switching techniques to this converter will improve the overall efficiency.

Acknowledgment

The authors would like to thank the Public Authority for Applied Education and Training (PAAET) for supporting this work through project no: TS-04-004.

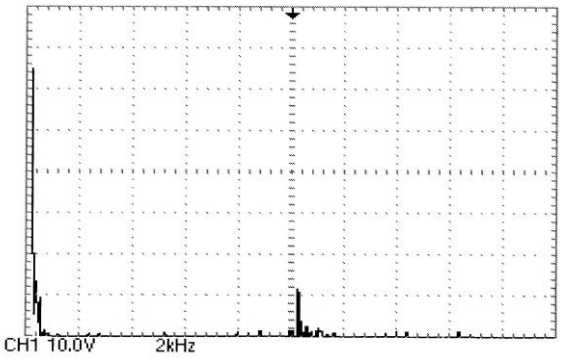

Fig. 19. Harmonic spectrum of the output line voltage.

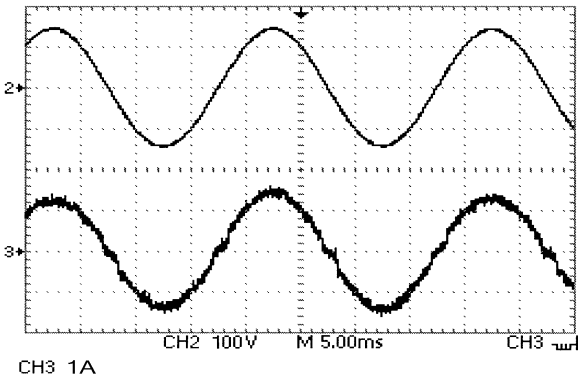

Fig. 20. The supply input phase voltage and current.

Appendix (a)

The Simulink connection diagram and subsystems

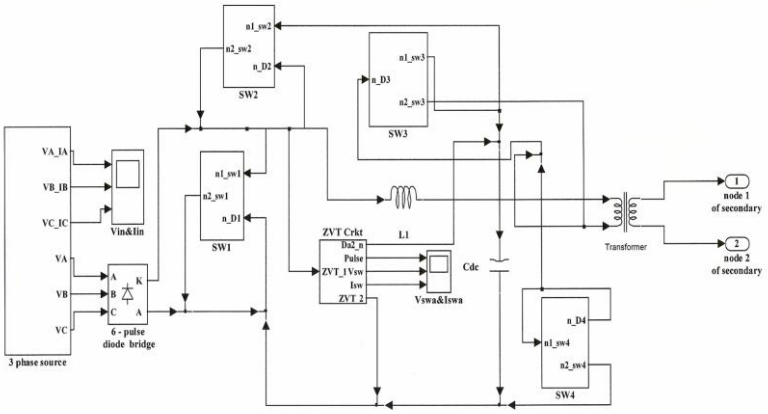

3-ph boost integrated ZVT bridge converter

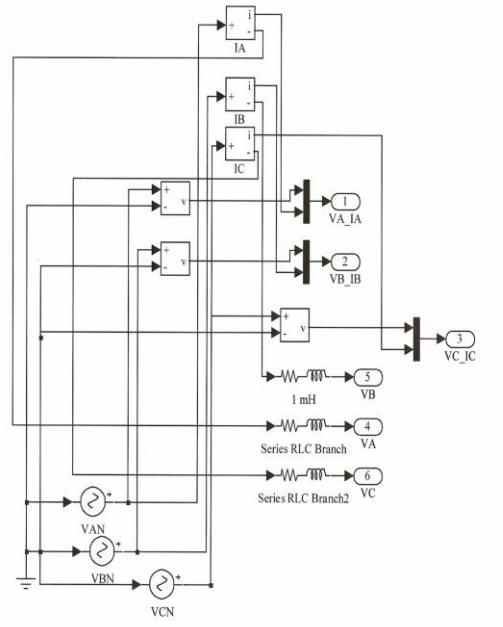

3-ph supply input subsystem

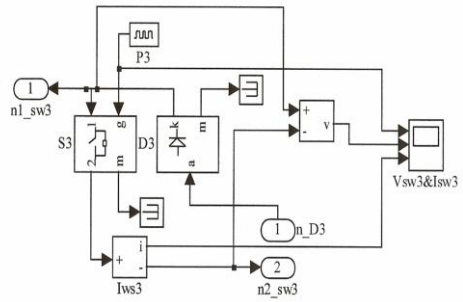

ZVT bridge converter switch subsystem

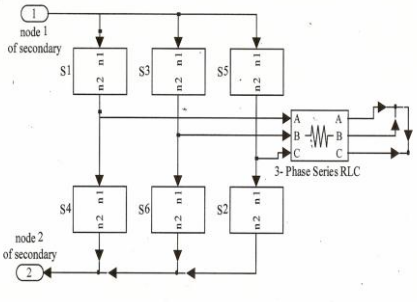

1-ph to 3-ph AC-AC converter

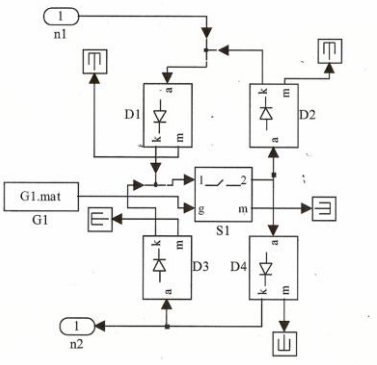

Bi-directional switch subsystem

References

[1] D. Van der Berg and J.A. Ferreira, "A Family of Low EMI Unity Power Factor Converters", IEEE Trans. Power Electron., Vol. 13, pp. 547-555 (1998).

[2] J.M. Garcia, J.A. Cobos, R. Prieto, P. Alou and J. Uceda, "Power Factor Correction: A Survey", in Proc. IEEE PESC'01, pp. 8-13 (2001).

[3] H. Yu, B.M. Song and J.S. Lai, "Design of a Novel ZVT Soft-Switching Chopper", IEEE Trans. Power Electron., Vol. 17, pp. 101-108 (2002).

[4] C.M. Duarte and Barbi, "A Family of ZVS-PWM Active Clamping DC-to-DC Converters: Synthesis, Analysis, Design, and Experimentation", IEEE Trans. Circuits Syst. 1, Vol. 44, pp. 698-704 (1997).

[5] T.W. Kim, H.S. Kim and H.W. Ahn, "An Improved ZVT PWM Boost Converter", in Proc. IEEE PESC'00, pp. 615-619 (2000).

[6] T. Wu, S. Liang and Y. Chen, "A Structural Approach to Synthesizing Soft Switching PWM Converters", IEEE Trans. Power Electron., Vol. 18 (1), pp. 38-43 (2003).

[7] G. Hua and F.C. Lee, "Soft Switching Techniques in PWM Converters", IEEE Trans. Ind. Electron., Vol. 42, pp. 595-603 (1995).

[8] A. Elasser and D.A. Torry, "Soft Switching Active Snubbers for dc/dc Converters", IEEE Trans. Power Electron., Vol. 11, pp. 710-722 (1996).

[9] C.J. Tseng and C.L. Chen, "Passive Lossless Snubbers for dc/dc Converters", in Proc. IEEE APEC'98, pp. 1049-1054 (1998).

[10] J.G. Cho, J.W. Baek, G.H. Rim and I. Kang, "Novel Zero-Voltage-Transition PWM Multiphase Converters", IEEE Trans. Power Electron., Vol. 13, pp. 152-159 (1998).

[11] W. Guo, P. K. Jain, "A Low Frequency ac to High Frequency AC Inverter with Building Power Factor Correction and Soft Switching", IEEE Trans. Power Electron., Vol. 19 (2), pp. 430-442 (2004).

Received June 25, 2006
Accepted February 11, 2007